PHYSICS AND RADIATION BIOLOGY

Radiation Dose Calculation for Tc-99m HIDA in Health and Disease

P. H. Brown, G. T. Krishnamurthy, V. V. R. Bobba, and E. Kingston

Veterans Administration Medical Center and University of Oregon Health Sciences Center, Portland, Oregon

Radiation dose from Tc-99m HIDA has been calculated for normal subjects and for patients with various hepatobiliary diseases classified into four groups based on serum bilirubin level. The calculation was performed on biokinetic radioactivity data from blood, urine, liver, gallbladder, and intestines, using a biological approach that included a catenary model of the digestive organs. For normal subjects the critical organs were the gallbladder and the upper and lower large intestine, with doses of 910, 300, 200 mrad/mCi, respectively. The bone marrow, ovaries, and testes received 24, 62, and 4 mrad/mCi. For Group 4 patients with severe hepatobiliary disease (bilirubin >10 mg/dl), the critical organs were the kidney, urinary bladder, and gallbladder, with doses of 130, 110, and 100 mrad/mCi. The bone marrow, ovaries, and testes received 9, 13, and 5 mrad/mCi. Thus the critical organs and overall radiation doses to organs change between health and disease.

J Nucl Med 22: 177–183, 1981

Hepatobiliary imaging has assumed an increasing role in nuclear medicine in recent years since the introduction of Tc-99m-labeled analogs of iminodiacetic acid (*1*). The clinical role of these agents has recently been reviewed (*2,3*). With this wider clinical application it is essential to establish human radiation dosimetry for these agents. The radiopharmaceutical kit manufacturers currently project human dose calculations based mostly on data from animal studies (*4–6*). One published abstract of dose calculation for Tc-99m PIPIDA reported equal liver and gallbladder doses and did not list bladder dose (*7*). The present communication describes human dose calculation of Tc-99m HIDA (*4*) based on biological modeling and quantitative pharmacokinetic data collected in 15 normal subjects and in 25 patients with various hepatobiliary diseases. The biokinetic measurements include blood clearance and urinary excretion, hepatic uptake and excretion rates, and gallbladder ejection fraction following a fatty meal (*8,9*).

Received May 13, 1980; revision accepted Oct. 31, 1980.

For reprints contact: Paul H. Brown, Nuclear Medicine Service, VA Medical Ctr., 3710 SW U.S. Vet. Hosp. Rd, Portland, OR 97201.

MATERIALS AND METHODS

Fifteen healthy adult volunteers for normal controls (NC), and 25 patients with liver disease, were studied. The patients were divided into four groups based on their serum level of total bilirubin. Group 1 patients (n = 9) had bilirubin levels within normal limits, with a mean of 0.7 mg/dl; in Group 2 (n = 6) the range was 1–5 mg/dl (mean = 2.1 mg/dl); in Group 3 (n = 5) it was 5–10 mg/dl (mean = 7.6 mg/dl); and in Group 4 (n = 5) the bilirubin was >10 mg/dl (mean = 14 mg/dl). After an overnight fast, each subject was given 5 mCi of Tc-99m HIDA (*4*) intravenously. Serial analog images of the liver and gallbladder (GB) were obtained at 1-min intervals for 60 minutes with a large-field gamma camera, fitted with a low-energy, high-resolution, parallel-hole collimator and interfaced to a computer in 64 × 64 matrix mode. Ninety minutes after injection of Tc-99m HIDA, gallbladder (GB) images were obtained at 1-min intervals for another 60 min using a 5-mm pinhole collimator. Ten minutes after beginning the study with the pinhole collimator, fatty milk (220 cc/70 kg) was given orally to allow measurement of the GB ejection fraction (*8,9*). Blood and urine samples for

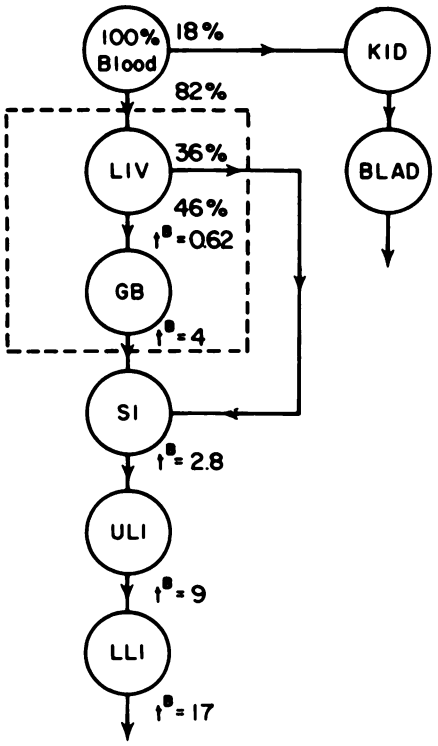

FIG. 1. Biological model used for Tc-99m HIDA dose calculation in normal controls. Blood activity is modeled with a 3-component exponential. Percent of dose excreted in urine is measured and modeled as shown in Fig. 2. Activity not excreted in urine leaves the blood and enters a catenary model beginning with liver and ending with lower large intestine.

measurement of blood clearance and urinary excretion were collected, at intervals as noted below, for 24 hr.

The radiation dose was calculated by the MIRD method (*10,11*) in which the absorbed dose $D(r_k \leftarrow r_h)$ in rad to a target organ, r_k, due to activity in a source organ, r_h, is given by:

$$D(r_k \leftarrow r_h) = \tilde{A}_h S(r_k \leftarrow r_h) \qquad (1)$$

where $\tilde{A}_h$ is the cumulated activity in the source organ and $S(r_k \leftarrow r_h)$ is the absorbed dose per unit cumulated activity from MIRD Pamphlet No. 11 (*11*). The cumulated activity in the source is obtained by integration of the source-organ activity over all time. Then the total dose to a target organ is determined by summing the dose to the target organ from each of the source organs. Here, as shown in Fig. 1, the source organs were blood, kidney, urinary bladder, liver, GB, small intestine, and upper and lower large intestine. Since the GB is not a source organ in the MIRD formulation, it was necessary to use special calculations for the GB as a source organ. In the results given below, the cumulated activity per mCi of injected dose was calculated for each source organ, and the radiation doses to the target organs were then calculated. The activity data for the source organs were fitted with mathematical functions to facilitate the integration necessary to find the cumulated activity, but it is not the intent here to attribute physiological significance to any of these mathematical models.

RESULTS

Bladder cumulated activity. The HIDA was injected into fasting subjects at 9:00 a.m., and urine samples were obtained at 1, 3, and 24 hr after injection. These samples were counted against a prepared standard to determine the percent dose of HIDA in urine. The 1- and 3-hr samples were single urine samples, whereas the 24-hr sample was a cumulative collection obtained by the subject between 3 and 24 hr. The 24-hr sample was presumed to consist of four aliquots obtained by the subject at postinjection times of 7, 11, 15, and 24 hr, consistent with the remainder of the day followed by a 9-hr sleep interval. The percentages in these aliquots were presumed to be 3/4, 1/8, 1/16, and 1/16 of the 24-hr sample, respectively. Assigning most of the 24-hr

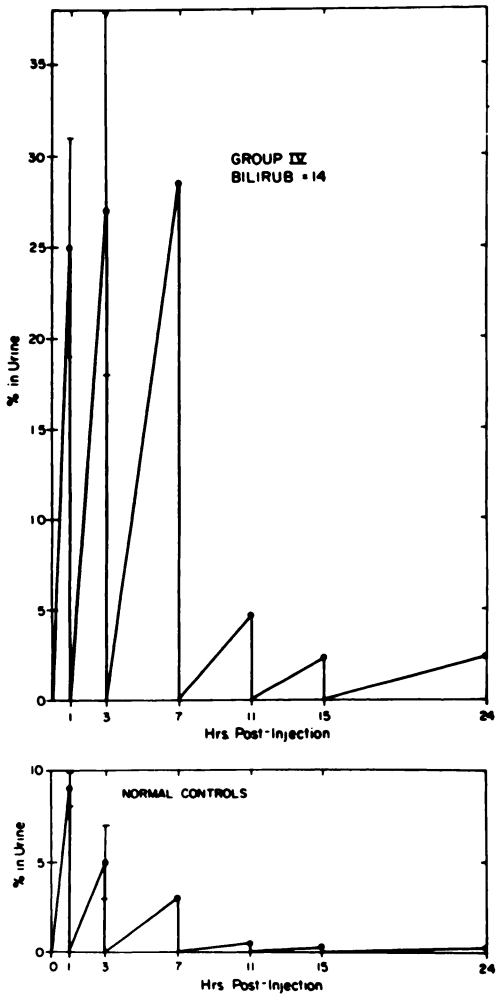

FIG. 2. Percent Tc-99m HIDA excreted in urine, against time after injection, for normal controls and Group 4 patients. First two samples are shown with ± std. error bars, and last four points are modeled as noted in text. Triangular areas represent model's handling of urine in urinary bladder.

TABLE 1. Tc-99m HIDA CUMULATED ACTIVITY IN μCi-hr PER mCi OF INJECTED DOSE

Source organ	Group				
	Control	1	2	3	4
Urinary bladder	117	207	263	502	672
Kidney	117	207	263	502	672
Blood	185	362	330	598	610
Liver	660	1190	1290	630	204
Gallbladder	1460	1130	940	470	150
Small intestine	1831	1406	1181	581	188
Upper large intestine	1904	1464	1230	604	195
Lower large intestine	934	718	603	297	96

sample value to the earlier aliquots preserves a conservative dose calculation while still allowing realistically for bladder emptying. A model of urine production was assumed in which urine activity increased in the bladder linearly in time until urination, at which time bladder activity in theory dropped to zero. A graphic representation of the urinary data is shown in Fig. 2 for the two extreme cases of a normal control and the Group 4 patients. These data were corrected for physical decay to represent biological excretion only. Thus when physical decay is considered, the later urine aliquots become increasingly unimportant to the calculation of cumulated activity. The triangular areas in Fig. 2 were multiplied by the physical decay constant and integrated to obtain the cumulated activity.

$$\tilde{A}_{BL}(\mu\text{Ci-hr}) = (1000\ \mu\text{Ci}) \sum_{i=1}^{6} \int_{t_{1i}}^{t_{2i}} (e^{-\lambda t})(a_i + b_i t)dt$$

where t_{1i}, t_{2i}, a_i, and b_i are, respectively, the starting and ending time in hours, the y intercept in fraction of dose, and the slope in fraction of dose/hr for the six triangles shown in Fig. 2. The results are shown in Table 1. The cumulated activity in the urinary bladder for Group 4 patients was more than five times that of normal controls, showing the increasing importance of the bladder as an excretion route for HIDA as bilirubin rises.

A model used previously for Tc-99m DTPA dose calculation (*12*) was similar in that it also assumed repeated bladder filling and emptying. However, this DTPA model assumed a single exponential removal of activity from the blood into the kidney, which is not the case for HIDA (because of liver-kidney competition for HIDA), and required knowledge of a urine production rate. There are other assumptions, besides the triangular model used here, that may be made concerning the shape of the bladder's filling curve, but the data here (three urine samples) cannot distinguish between the various possible shapes. The use of cumulated bladder activity—based on changing bladder volume in conjunction with S factors that assume a constant-volume organ—is one of the hazards involved in the use of S factors in dosimetry calculations. Because of these considerations, the bladder and kidney doses calculated here are felt to be less accurate than the doses calculated for other organs, but the change in these doses from normal controls to high bilirubin patients remains valid. The dose estimate presented here rests on experimentally measured urine activity with assumptions of urine production as stated.

Kidney (KI) cumulated activity. Since no data were accumulated directly from the kidney, it was necessary to infer the cumulated kidney activity from other data. One method is to assume the kidney cumulated activity to be equal to the urinary-bladder value; this overestimates the kidney exposure since the activity leaves the kidney at a rate faster than it leaves the bladder, due to buildup in the bladder with negligible delay in ureter transit time. This conservative and simple approach was adopted here. Other assumptions are possible but not necessarily more accurate. A manufacturer of PIPIDA (*5*) calculates kidney cumulated activity by measuring a simple effective half-life from urinary bladder data and arbitrarily assigning this half-life solely to the kidney. This model does not allow bladder emptying or storage of urine and is more artificial and nonphysiological than the model used here.

Blood cumulated activity. The activity in the blood was considered to be distributed uniformly throughout the body, so that the blood was used as a total-body (TB) source in the MIRD formulation. The blood data, corrected for physical decay, were well fitted by a three-component (slow, medium, fast) exponential:

$$A_{TB}(t) = \sum_{i=1}^{3} A_i e^{-0.693t/t_i^b}$$

where A_i is the fraction of the dose at t = 0, and t_i^b is the biological half-life for the i-th component. The A_i and t_i^b values (Table 2) were determined by an unweighted, nonlinear, least-squares fitting program (*13,15*) that has been developed to run on a nuclear medicine minicomputer. The standard error of the estimate (*14*)—a measure of the deviation between the fit and the data values—is also shown in Table 2. The blood data, with ±1 s.e. bars and the curve fit, are shown in Fig. 3 for the normal controls and the group of patients with highest bilirubin. The activity is multiplied by the physical decay factor and integrated to give the cumulated activity (Table 1), which rises rapidly with increasing bilirubin.

Liver cumulated activity. During the first hour after injection, liver radioactivity was defined by a computer region of interest over the superolateral liver border in order to exclude the bile-collection system. Using Tc-99m diethyl-IDA in severe liver disease (*16*), it has been shown that as bilirubin rises, the liver curve changes shape from an exponential uptake-excretion function to a shape much like that of the blood data: a bolus uptake

TABLE 2. PARAMETERS OF THE BLOOD MODEL: PERCENT ACTIVITY OF Tc-99m HIDA AT t = 0, AND BIOLOGICAL HALF-LIFE FOR THE THREE COMPONENTS OF THE EXPONENTIAL FIT

	Slow		Medium		Fast		
Group	A_1 (%)	t_1^b (min)	A_2 (%)	t_2^b (min)	A_3 (%)	t_3^b (min)	Std. err. est.
Control	1.70	1300	17.1	17.2	14.0	2.85	0.82
1	3.55	3970	18.5	16.4	39.3	1.07	0.96
2	3.28	935	13.5	34.6	47.1	1.94	1.03
3	8.00	684	15.4	37.7	29.4	2.74	0.89
4	6.81	675	16.6	60.0	19.4	4.62	1.05

followed by slower excretion. This is due to increased blood radioactivity as bilirubin rises secondary to decreased hepatocyte function. To account for this, a blood background was subtracted from the liver data by subtracting counts per pixel from a region of interest over the spleen, where HIDA does not localize. The background-corrected liver data were also corrected for physical decay, and these data were found to be well fitted by a simple uptake-excretion, two-component exponential,

$$A_{LIV}(t) = C(e^{-\lambda_{ex}^b t} - e^{-\lambda_{up}^b t}),$$

by an unweighted least squares fit, with a rapid uptake followed by a slower excretory biological half-life. This is shown for a typical normal control (NC) and a typical Group 3 patient (bilirubin = 8) in Fig. 4.

The results for all groups are tabulated in Table 3. Note that these data were derived from subjects other than those used for blood data, so the n values are different. It can be seen in Table 3 that the excretion half-lives have standard errors that range from 10% in normal controls to 40% in Group 2 patients because of their wide range of disease states. As bilirubin rises, the urinary and blood activities rise rapidly and the activity in the liver becomes increasingly less important for dosimetry. For patients in Groups 3 and 4, for example, 70 and 90% of the dose is excreted in urine, leaving only 30 and 10% to be excreted in bile. Because of the small number of counts, the liver curves for patients in these groups were not well fitted by the uptake-excretion model. The excretion half-lives for Groups 3 and 4 patients, therefore, were arbitrarily taken to be the same as in Group 2.

The rapid biological half-life (5 min) for liver uptake compared with the biological excretion half-life (37 min or more), suggests that the dose calculation can be conservatively simplified by assuming instantaneous liver uptake and by assuming—since the only known excretion routes for Tc-99m HIDA are the renal and hepatobiliary systems (*1*)—that all the activity not excreted by the kidneys within 24 hr was localized in the liver at time zero. The activity subsequently leaves the liver with the measured biological excretion half-life, as shown in Table 3. Note that the subtraction of blood background affects only the half-life value and not the determination of percent of dose that localizes in the liver, which was determined as 100% minus total urinary excretion. The digestive-tract organs were modeled by considering the liver to be the first compartment in the catenary model shown in Fig. 1. The equations describing such a model have been described previously (*17*). Figure 5 shows the liver prediction of the model for normal controls. These liver data were integrated over all time to find the cu-

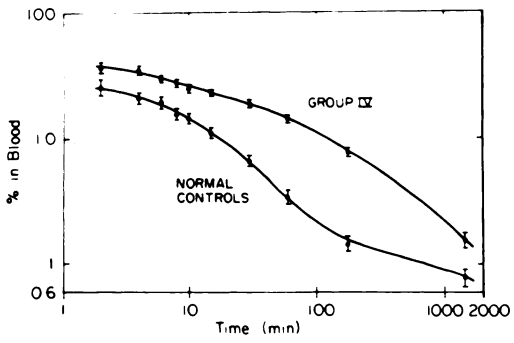

FIG. 3. Percent dose of Tc-99m HIDA in blood, against hours after injection, for normal controls and Group 4 patients, shown with ± standard error bars and three-component exponential curves for least-squares fit. Note statistically significant higher blood levels in Group 4 patients ($p < 0.001$ for all data points).

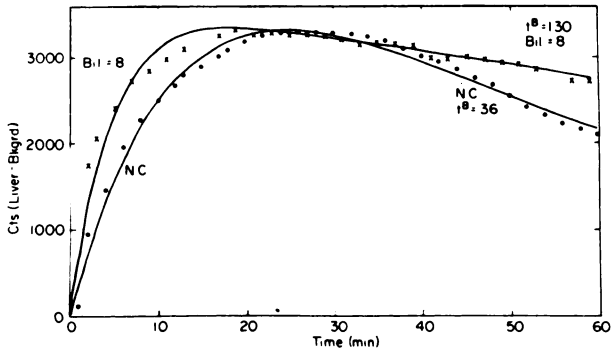

FIG. 4. Background-subtracted liver curve for normal control and Group 3 patient with total bilirubin 8 mg/dl. Curves are least-squares uptake-excretion exponential fits, with biological excretion time in minutes. Note prolonged excretion half-time of 130 min in a Group 3 patient, against 36 min in a normal control.

TABLE 3. Tc-99m HIDA LIVER EXCRETION AND UPTAKE BIOLOGICAL HALF-LIFE (± s.e.m.) FROM THE LEAST-SQUARES FIT

Group	t^b_{ex} (min)	t^b_{up} (min)
Control, n = 23	36.9 ± 2.8	5.7 ± 1.4
1, n = 11	87 ± 24	5.5 ± 0.7
2, n = 5	112 ± 47	5.2 ± 0.5
3	112	5.2
4	112	5.2

mulated activity (Table 1), which reflects the decreasing localization of HIDA in the liver as bilirubin rises.

Gallbladder cumulated activity. Computer regions of interest were placed over the GB, minus a liver background region, and over all of the intestines during the 60-min frame of the study. The net GB counts were defined as (GB counts − background), and the total counts were defined as (net GB counts + intestine counts). Then the percentage of liver activity going to the GB was defined as (net GB counts/total counts), and the percentage going to intestines was defined as (intestine counts/total counts). The results for normal controls were that the activity leaving the liver divides, with (56 ± 8)% (mean ± s.e.m.) going to the GB and (44 ± 8)% passing directly into the small intestine (SI). In normal controls, the GB biological excretion half-life was measured as 4 hr, based on a 6-hr meal schedule, and a GB ejection fraction of 65% following a fatty meal (*8,9*). Patients were assumed to have the same GB parameters as normal controls. The solution for the second compartment, the GB, in the catenary model has been described previously (*17*). Figure 5 shows the GB predictions of the model for normal controls, with Compartment No. 1 values as noted in liver discussion above, and t^b_2 = 4 hr. The cumulated GB activity (Table 1) shows that, in Group 4 patients, the combination of slower liver excretion and less activity in the liver, as bilirubin rises, results in a fall of the cumulated activity to one-tenth of the normal control value.

Small intestine (SI) cumulated activity. The SI receives activity directly from the liver and also from the GB when it contracts, as discussed above. For the 56% of the liver activity that enters the SI through the liver-GB-SI route, the SI is the third compartment in the model, whereas it is the second compartment for the 44% of the liver activity that bypasses the gallbladder. The calculation of cumulated activity (see Table 1) from these two contributions was straightforward, by integrating the model equations (*17*) for the second and third compartments and adding these two contributions. The biological excretion half-life from the SI has been determined to be 2.8 hr (*17,18*). Figure 5 shows the model

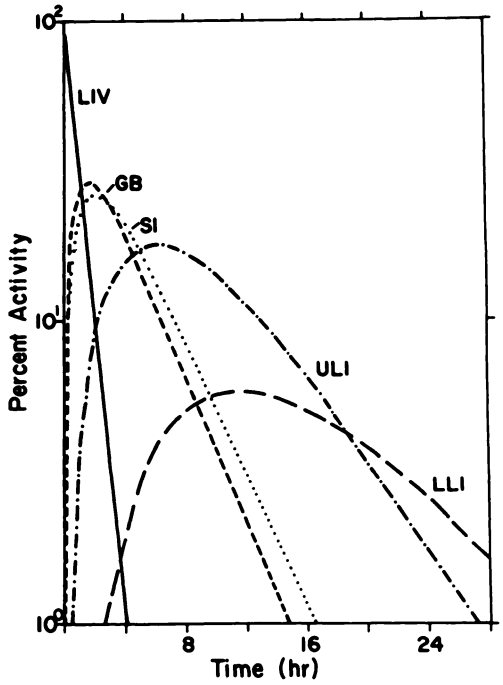

FIG. 5. Predictions for a normal subject (catenary model, Fig. 1) for liver (LIV), gallbladder (GB), small intestine (SI), upper large intestine (ULI), and lower large intestine (LLI). Cumulated Tc-99m HIDA activities are calculated by integrating these data.

predictions for these SI data in normal controls, and Table 1 shows that the SI cumulated activity shows a decrease to one-tenth from normal controls to high-bilirubin patients, like the behavior of the GB cumulated activity. Because of the longer biological half-life of the GB compared with the liver, the SI receives approximately two thirds of its cumulated activity from activity that enters the SI directly from the liver, and the remaining one third is from activity through the liver-GB-SI route.

Cumulated activity for the upper and lower large intestine (ULI and LLI). This was calculated in a similar fashion, by using biological half-lives of nine and 17 hr for the ULI and LLI (*17,18*), and by adding the contributions from activity that passed through and bypassed the GB. The cumulated activity is shown in Table 1, and Fig. 5 shows model predictions for the ULI and LLI in normal controls. The cumulated activity varies with bilirubin in a fashion similar to that for the SI, but the contributions to be summed for the liver and liver-GB routes are approximately equal, due to the long half-lives in the intestines.

Absorbed dose. The calculation of absorbed dose was straightforward, utilizing Eq. 1 with the cumulated activities in Table 1, accepting the GB and liver as either target or source organs. The target organs chosen here are listed, with the results, in Table 4. The liver and GB must be considered separately since activity in the GB is not considered in the MIRD formulation of Eq. 1. The method chosen for these calculations was the same as

that reported previously for radioiodine sodium rose bengal (*19*).

The doses to target organs other than the liver or GB, due to activity in the liver and GB, were calculated by summing the cumulated activities in the liver and GB and using Eq. 1 with an S factor for the liver as the source:

$$D(\text{target} \leftarrow \text{LIV} + \text{GB}) = (\tilde{A}_{LIV} + \tilde{A}_{GB})S(\text{target} \leftarrow \text{LIV})$$

where target is not LIV or GB.

The liver was considered as a target, with source organs other than the GB, by straightforward applications of Eq. 1. The dose to the liver from the gallbladder contents (GBC) was taken as the penetrating (p) dose from the GBC, using the absorbed fraction for dose to the liver from the liver (*20,21*):

$$D(\text{LIV} \leftarrow \text{GBC}) = (\tilde{A}_{GBC}/m_{LIV}) \sum_{i,p} \Delta_i \phi_i(\text{LIV} \leftarrow \text{LIV})$$

This technique, of using ϕ (LIV ← LIV) instead of the (unavailable) ϕ(LIV ← GBC), will overestimate the liver dose. The nonpenetrating radiation from the GBC is absorbed in the gallbladder wall (GBW).

Next, consider the GBW as the target. The dose to the GBW, from sources other than the liver and GBC, was calculated from $\tilde{A}_{source}$ using the absorbed fraction for the liver as the target. The dose to the GBW from the LIV and GBC was divided into penetrating (p) and nonpenetrating (np) components. The dose to the GBW from the penetrating radiation was taken as the penetrating dose to the liver from the liver, plus the penetrating dose to the GBC from the GBC:

$$D(\text{GBW} \leftarrow \text{LIV} + \text{GBC})_p = D(\text{LIV} \leftarrow \text{LIV})_p + D(\text{GBC} \leftarrow \text{GBC})_p$$

$$= (\tilde{A}_{LIV}/m_{LIV}) \sum_{i,p} \Delta_i \phi_i(\text{LIV} \leftarrow \text{LIV}) + (\tilde{A}_{GBC}/m_{GBC}) \sum_{i,p} \Delta_i \phi_i(\text{GBC} \leftarrow \text{GBC})$$

The equilibrium dose constants and liver absorbed fractions are published (*20,21*), whereas the gallbladder values are not part of the MIRD formulation. The GB size was taken as 50 ml (*22*), and it was assumed to be an ellipsoid to allow use of MIRD published absorbed fractions (*23*) for gamma-2 and gamma-3 (*21*). The absorbed fraction, ϕ (GBC ← GBC), for the K x-rays was estimated as 0.6. The nonpenetrating dose to the GBW was calculated by the usual MIRD technique for organs with walls (*11*), except that here the GBW also receives np radiation from the liver.

$$D(\text{GBW} \leftarrow \text{LIV} + \text{GBC})_{np} = 0.5D(\text{LIV} \leftarrow \text{LIV})_{np} + 0.5D(\text{GBC} \leftarrow \text{GBC})_{np}$$

$$= (0.5\tilde{A}_{LIV}/m_{LIV}) \sum_{i,np} \Delta_i + (0.5\tilde{A}_{GBC}/m_{GBC}) \sum_{i,np} \Delta_i$$

TABLE 4. ABSORBED DOSE IN mrad/mCi OF Tc-99m HIDA

Target organ	Group				
	Control	1	2	3	4
Urinary bladder wall	35	46	53	87	111
Bone	9	9	8	6	4
Gallbladder wall	908	728	617	309	101
Small intestine	189	147	125	65	25
Upper large intestine	302	235	198	100	36
Lower large intestine	199	154	131	68	27
Kidney	43	58	67	105	132
Liver	76	91	90	47	18
Marrow	24	21	19	13	9
Ovaries	62	50	43	25	13
Spleen	9	8	7	5	3
Testes	4	4	4	4	5
Total body	16	15	14	9	6

In addition to this method for the calculation of dose to the GBW, it is now possible to use calculated S factors for S(GBW ← source) (*26*). Using these with the cumulated activities for normal controls in Table 1, we obtain a dose to the GBW of 773, compared with the 908 mrad/mCi (Table 4) calculated here by methods postulated to be conservative.

DISCUSSION

The data in Table 4 show that for normal controls the critical organs were GB, ULI, LLI, SI, and liver, in order of decreasing dose, as is expected for a hepatobiliary agent. The normal controls for this study were typically given 5 mCi, but diagnostically useful biliary images can be obtained in patients with normal bilirubin levels with as little as 2-3 mCi of Tc-99m HIDA. As bilirubin rises, the critical organs changed and the kidneys became the primary route of excretion. For Group 4 patients (bilirubin >10 mg/dl), for example, the critical organs in order of decreasing dose were kidney, urinary bladder, and gallbladder, with the other organs receiving <36 mrad/mCi. Since the dose to the GB and intestines dropped markedly at higher bilirubin levels, it appears that the radioactivity given to jaundiced patients could be increased to compensate for low liver uptake, while still serving the clinical need of adequate visualization of the biliary tree. The radiation dose to the urinary bladder and other nearby organs may be minimized by encouraging patients to urinate frequently after injection of the HIDA.

A dose calculation for TC-99m PIPIDA appears in an abstract (*7*), based on six normal subjects. It gives equal liver and gallbladder doses of 200 mrad/mCi, which indicates that gallbladder concentration and storage of activity was not considered. A bladder dose is not listed. Other dose calculations for Tc-99m imi-

nodiacetic acid analogs (*4–6*) are unpublished manufacturer's literature, which use varying, often unspecified, assumptions about biokinetic parameters, and may list doses above or below those reported here. Before the introduction of iminodiacetic acid analogs, I-131 rose bengal was the agent used for hepatobiliary imaging, with dose estimates (*19*) of 1100 mrad/mCi to the gallbladder and 800 mrad/mCi to the liver. These estimates are not directly comparable to the data reported here, since the rose bengal doses are based on biokinetic parameters that were estimated from inspection of scintiphotos. Specifically, the rose bengal visual estimations (*19*) ignored kidney concentration of rose bengal (*25*) and reported higher liver localization and lower gallbladder localization then our data do. We believe that our results, based on quantitative computer data, are more accurate than the visual estimates with rose bengal. Oral cholecystography is an alternative procedure for evaluating gallbladder function; for a typical study consisting of 1 min of fluoroscopy, a prone PA, and a prone oblique radiograph, it delivers doses of 17 mrad to the testes and 78 mrad to the ovaries, with a surface dose of 945 mrad (*24*).

ACKNOWLEDGMENT

This work was supported by the U.S. Veterans Administration.

REFERENCES

1. LOBERG MD, COOPER M, HARVEY E, et al: Development of new radiopharmaceuticals based on N-substitution of iminodiacetic acid. *J Nucl Med* 17:633-638, 1976
2. SILBERSTEIN EB: Still more applications of hepatobiliary scintigraphy. *J Nucl Med* 21:99-100, 1980
3. EIKMAN EA: Radionuclide hepatobiliary procedures: when can HIDA help? *J Nucl Med* 20:358-361, 1979
4. Package insert for Tc-99m-HIDA, MPI hepatobiliary reagent, Medi-Physics Co., Emeryville, CA
5. Package insert for Tc-99m-PIPIDA, Diagnostic Isotopes Inc., Bloomfield, NJ
6. Package insert for Amersham Tc-99m-EHIDA kit, Amersham Corp., Arlington Heights, IL
7. WILLIAMS LE, PONTO RA, FORSTROM LA, et al: Human dosimetry of Tc-99m PIPIDA. *J Nucl Med* 20:607, 1979 (abst)
8. KRISHNAMURTHY GT, BOBBA VVR, KINGSTON E, et al: Ejection fraction: A new objective method of studying motor function of the gall bladder. *J Nucl Med* 20:632, 1979 (abst)
9. KRISHNAMURTHY GT, BOBBA VR, KINGSTON E: Radionuclide ejection fraction: A new technique for quantitative analysis of motor function of the human gallbladder. *Gastroenterology*, in press
10. LOEVINGER R, BERMAN M: A revised schema for calculating the absorbed dose from biologically distributed radionuclides. MIRD Phamphlet No. 1, Revised, New York, Society of Nuclear Medicine, 1976
11. SYNDER WS, FORD MR, WARNER GG, et al: "S" absorbed dose per unit cumulated activity for selected radionuclides and organs, MIRD Pamphlet No. 11, New York, Society of Nuclear Medicine, 1975, pp
12. DIFFEY BL, HILSON AJ: Absorbed dose to the bladder from Tc-99m-DTPA. *Br J Radiol* 49:196-198, 1976
13. BEVINGTON PR: *Data Reduction and Error Analysis for the Physical Sciences.* New York, McGraw Hill Co., 1969, pp 232-246
14. COLTON T: *Statistics in Medicine.* Boston, Little Brown and Co., 1974, p 198
15. SIMON W: *Mathematical Techniques for Biology and Medicine.* Cambridge, MIT Press, 1977, pp 231-237
16. NIELSEN SP, TRAP-JENSEN J, LINDENBERG J, et al: Hepato-biliary scintigraphy and hepatography with Tc-99m diethyl-acetanilido-iminodiacetate in obstructive jaundice. *J Nucl Med* 19:452-457, 1978
17. BERNARD SR, HAYES RL: Dose to various segments of the gastrointestinal tract. In medical radionuclides: radiation dose and effects, proceedings of a symposium Oak Ridge Associated Universities, Dec. 1969, Conf. 691212, U.S. National Technical Information Service, Springfield, VA, 1970, pp 295-314
18. EVE IS: A review of the physiology of the gastrointestinal tract in relation to radiation doses from radioactive materials. *Health Phys* 12:131-161, 1966
19. MIRD Dose Estimate Report No. 7: Summary of current radiation dose estimates to humans from 121-I, 124-I, 126-I, 130-I and 131-I as Sodium Rose Bengal. *J Nucl Med* 16: 1214-1217, 1975
20. SNYDER WS, FORD MR, WARNER GG: Estimates of absorbed fractions for monoenergetic photon sources uniformly distributed in various organs of a heterogeneous phantom. MIRD Pamphlet No. 5, New York, Society of Nuclear Medicine, 1969
21. DILLMAN LT, VON DER LAGE FC: Radionuclide decay schemes and nuclear parameters for use in radiation dose estimation. MIRD Pamphlet No. 10, New York, Society of Nuclear Medicine, 1975
22. BROBECK JR: *Best and Taylors Physiological Basis of Medical Practice.* 10th ed., Baltimore, Williams and Wilkins, 1979, pp 2-79
23. ELLET WH, HUMES RM: Absorbed fractions for small volumes containing photon-emitting radioactivity. MIRD Pamphlet No. 8, New York, Society of Nuclear Medicine, 1971, Table 7, p 30
24. BROWN RF, SHAVER JW, LAMEL DA, et al: The selection of patients for x-ray examinations. HEW Publication FDA-80-8104, U.S. Department of Health, Education and Welfare, Bureau of Radiological Health, Rockville, MD, 1980, p 31
25. WISTOW BW, SUBRAMANIAN G, VAN HEERTUM RL, et al: An evaluation of ^{99m}Tc labeled hepatobiliary agents. *J Nucl Med* 18:455-461, 1977
26. BERNARD SR, CHEN SM: Dose to the gallbladder from a 99m-Tc labeled gallbladder scanning agent. Proceedings Third International Radiation Dosimetry Symposium, October, 1980, Oak Ridge National Laboratory, Oak Ridge, TN.